Int. J. Electrochem. Sci., 11 **(2016)** 4550 – 4559, doi: 10.20964/2016.06.13

International Journal of
ELECTROCHEMICAL
SCIENCE
www.electrochemsci.org

Biosynthesis of Gold Nanoparticles Using Green Alga *Pithophora oedogonia* with Their Electrochemical Performance for Determining Carbendazim in Soil

Lei Li[1] *and Zunju Zhang*[2,*]

[1] Northeast Petroleum University at Qinghuangdao, No. 550 West of Hebei Rd, Haigang, Qinhuangdao, Hebei, 066004, P.R. China
[2] Environmental Management College of China, No. 8 Jingang Rd, Beidaihe, Qinhuangdao, Hebei, 066402, P.R. China
[*]E-mail: baxiannv1@126.com

Received: 3 March 2016 / *Accepted:* 8 April 2016 / *Published:* 4 May 2016

Biosynthesis nanomaterial have constituted a huge attention recently due to its non-toxic process. In this work, we demonstrated the biosynthesis of Au nanoparticles using green algae *Pithophora. oedogonia* as reducing agent. The entire synthesis process was rapid and the Au nanoparticles were formed within in 1 h after the Au salt reacted with algal extract. UV-vis spectroscopy and X-ray photoelectron spectroscopy were confirmed the formation of metallic state of Au. The average size of the biosynthesized Au nanoparticles was characterized to be 32.06 nm using scanning electron microscopy and dynamic light scattering machine. The biosynthesized Au nanoparticles were then used for screen printed electrode surface modification and showed an excellent electrocatalytic activity towards determination of carbendazim molecules in soil.

Keywords: Biosynthesis; Algae; Electrocatalysis; Sensor; Carbendazim

1. INTRODUCTION

Nanomaterial preparation is one of the most highly active research field in modern science [1, 2]. Synthesizing nanomaterials with controllable morphology and outstanding properties could make them applicable in many fields. Developing nanomaterials in the size range from 1 to 100 nm attracted most attention for researchers. Among them, preparation of metal nanoparticles have received extensive attention due to their distinct properties and wide potential applications including photocatalysis [3], sensing [4], supercapacitor [5], optoelectronics [6, 7], absorbent [8, 9] and thermal management [10, 11]. So far, metal nanoparticles are chemically prepared in nano-scale including

silver [12], gold [13], copper [14], zinc [15], titanium [16], cadmium [17], iron [18], palladium [19] and platinum [20]. Among the metals, gold nanoparticles showed promising performances in many potential applications including surface enhanced Raman spectroscopy [21], vapor sensing [22], catalysis [23], biosensor [24], drug delivery [25] and immunosensing [26]. Different types of approaches were developed for synthesizing Au nanoparticles including electro-deposition [27], chemical vapor deposition [28] and recently via green chemistry approach [29-41].

Biosynthesis of metal nanoparticle is an emerging branch of nanomaterial preparation. Different environmentally benign substances such as leaf extract, fungi, algae and bacterial were used as reducing agent for metal salt reduction. This approach provides numerous advantages such as eco-friendliness, high pharmaceutical compatibility and no toxic materials involved. Therefore, biosynthesis method has been found to be more superior than other chemical or physical based approaches. Au nanoparticles have been biosynthesized using ethanolic extract of *Brassica oleracea* L [29], bamboo (*Bambusa chungii*) leaf extracts [42], fungus *Penicillium chrysogenum* [43] and *Ficus racemosa* latex [44]. In this work, we proposed a new biosynthesis method for Au nanoparticles preparation using green alga *Pithophora oedogonia* as reducing agent. The synthesized Au nanoparticle was characterized using a series techniques for morphology and properties determination. Moreover, the biosynthesized Au nanoparticles also showed an excellent electrochemical property towards detection of carbendazim (methyl 1H-benzimidazol-2-ylcarbamate; see Figure 1 for its structure) in soil. This study provide an insight for potential electrochemical application based on the biosynthesized nanomaterial.

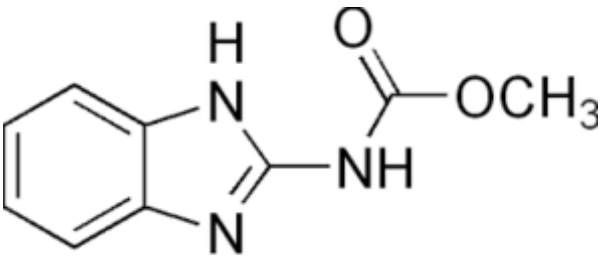

Figure 1. Chemical structure of the carbendazim.

2. EXPERIMENTS

2.1. Materials

All chemicals used in this study were of analytical grade brought from Sigma-Aldrich. Mill-Q water was used through the all experiment. The green algae *Pithophora oedogonia* was collected from the fresh pond in Northeast Petroleum University at Qinghuangdao. Fresh *Pithophora oedogonia* was then washed with Mill-Q water to remove extraneous impurity. The wet sample was the shade-dried for three days and then completely dried in a 70^{o}C oven. After drying, the *Pithophora oedogonia* sample was grounded into fine powder for further use.

2.2. Biosynthesis of Au nanoparticles using Pithophora oedogonia

10 g *Pithophora oedogonia* powder was added into 100 mL water and sonicated for 15 min and the heated to 70 ^{o}C for another 15 min. The *Pithophora oedogonia* extract was then filtrated using 200 nm pore size filter paper. The Au nanoparticles were synthesized adding 20 mL *Pithophora oedogonia* extract into 20 mL $HAuCl_4$ solution and sonicated for 1 h. The final solution turned from light yellow to purplish yellow, suggesting the formation of Au nanoparticles. Separation process was performed using centrifugation at 10,000 rpm for half hour followed by the wash cycle. Final Au nanoparticles were dried in a 70^{o}C oven.

2.3. Characterization

Scanning electron microscope (SEM, ZEISS X-MAX) was used for observing the morphology of biosynthesized Au nanoparticles. Elemental information of the sample was investigated using energy-dispersive X-ray spectroscopy (EDS). XRD pattern of the biosynthesized Au nanoparticles was collected from 10° to 80° in 2θ by a XRD (PW3040/60 X'pert PRO). The reduction of Au salt was confirmed using a UV-vis spectrophotometer (Shimadzu UV-1601PC) in the range of 300–800 nm. X-ray photoelectron spectroscopy (XPS, VGESCALAB MKII) was also used for confirming the formation of Au nanoparticles. A Malvern-Zeta-sizer (Nano-Z590) was used for dynamic light scattering (DLS) study of the size distribution of the biosynthesized Au nanoparticles.

2.4. Electrochemical determination of carbendazim

The electrochemical determination of carbendazim was performed using a three electrode system, which a saturated Ag/AgCl as a reference electrode and a Pt foil a counter electrode. The working electrode is a biosynthesized Au nanoparticles modified screen printed electrode (SPE). The SPE surface modification was carried out using following procedure: 0.1 mL biosynthesized Au nanoparticles (1 mg/mL) was dropped on the SPE surface and dried at room temperature. Electrochemical impedance spectroscopy (EIS) was used for characterizing the electrode surface electron transfer performance before and after modification. 5 mM $[Fe(CN)_6]^{3-/4-}$ was used as probe, 0.1 M KCl was used as supporting electrolyte. Frequency range was set as 10^1 to 10^5 Hz and the amplitude was set as 5 mV. Determination of carbendazim using CV method was performed at 0.1M PBS (pH = 7) at scan range between 0 to 1.0 V using scan rate of 50 mV/s.

2.5. Soil sample analysis

The biosynthesized Au nanoparticles modified SPE was used for analysing carbendazim in soil sample. Specifically, 500μL of the ethylene glycol/choline chloride mixture was added into 1 g soil sample in a Petri dish. After 15 min, the Au/SPE was inset into the soil sample and the linear sweep

voltammetry (LSV) method was applied for analytical determination. Standard addition method was applied for determination of carbendazim in soil samples.

3. RESULTS AND DISCUSSION

3.1. Characterization of biosynthesized Au nanoparticles

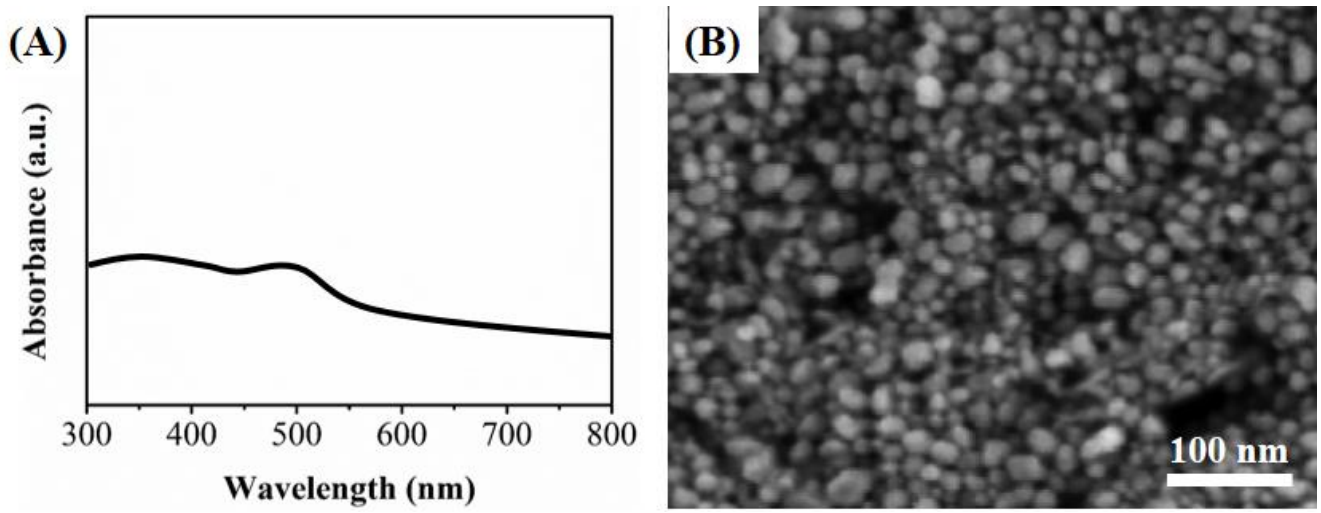

Figure 2. (A) UV-vis spectrum and (B) SEM image of biosynthesized Au nanoparticles.

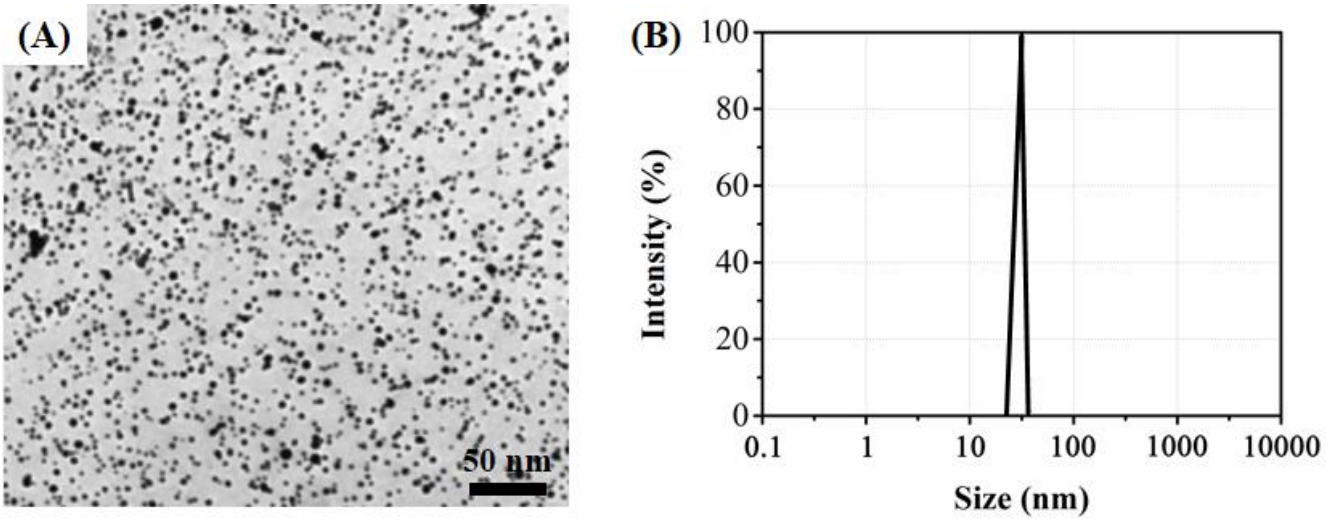

Figure 3. (A) TEM and (B) DLS pattern of biosynthesized Au nanoparticles.

During the experiment, the biosynthesis reaction started immediately when the *Pithophora oedogonia* extract added into the $HAuCl_3$ solution. The color of the dispersion slowly turned from light yellow to purplish yellow, suggesting the stating nucleation of Au nanoparticles. Surface plasmon resonances of the Au nanoparticles could be observed in the formed Au nanoparticle dispersion due to

the metallic nanoparticle could scatter and absorb light at a particular wavelength. The optical property of the Au nanoparticle could be affected by morphology, size and solvent. Figure 2A shows the UV-vis spectrum of Au nanoparticles synthesized using *Pithophora oedogonia*. In the spectrum, a distinct absorption peak can be noticed at 485 nm, corresponding to the surface plasmon resonance of the Au nanoparticles, which confirming the formation of metallic Au material. The surface plasmon resonance peak position can reflect the mean size of the formed Au nanoparticles. According to the literature, the size of the biosynthesized Au nanoparticles can be predicated in the range between 20 to 80 nm.

The morphology of the biosynthesized Au nanoparticles was characterized using scanning electron microscopy (SEM). As shown in Figure 2B, the biosynthesized Au nanoparticles displays a spherical shape with small aggregation. It can be observed that the size of the Au nanoparticles synthesized using *Pithophora oedogonia* seem uniform in size. Figure 3A shows the TEM image of the biosynthesized Au nanoparticles. Solid Au nanoparticles with an average size of 33 nm were observed. Most Au nanoparticles were in spherical shape, which is consistence with the SEM characterization. The size distribution of the Au nanoparticles was also characterized using DLS. As shown in Figure 3B, the DLS pattern displays the mean size distribution of Au nanoparticles was 32.06 nm. Moreover, the polydispersity index of the Au nanoparticles had been found to be 0.912, which could form a well dispersed colloidal solution.

The formation of Au nanoparticles was also confirmed using X-ray photoelectron spectroscopy. Figure 4A shows the Au_{4f} high resolution XPS scan for the biosynthesized Au nanoparticles. The $Au_{4f\ 7/2}$ and $Au_{4f\ 5/2}$ peaks were recorded on the 83.5 eV and 87.2 eV, respectively [45, 46]. The peaks showed a shift from theoretical value of Au^0 at 84.0 and 87.7 eV due to the surface attachment of biomolecules come from *Pithophora oedogonia* extract.

Figure 4B shows the XRD pattern of biosynthesized Au nanoparticles. The XRD spectrum of biosynthesized Au nanoparticles displays diffraction peaks located at 39.3°, 45.9°, 67.7° and 81.9°, corresponding to (111), (200), (220) and (311) planes of face-centered-cubic (fcc) crystallographic structure of Au (JCPDS 4-0783), respectively. The XRD result further confirmed the successful formation of metallic Au.

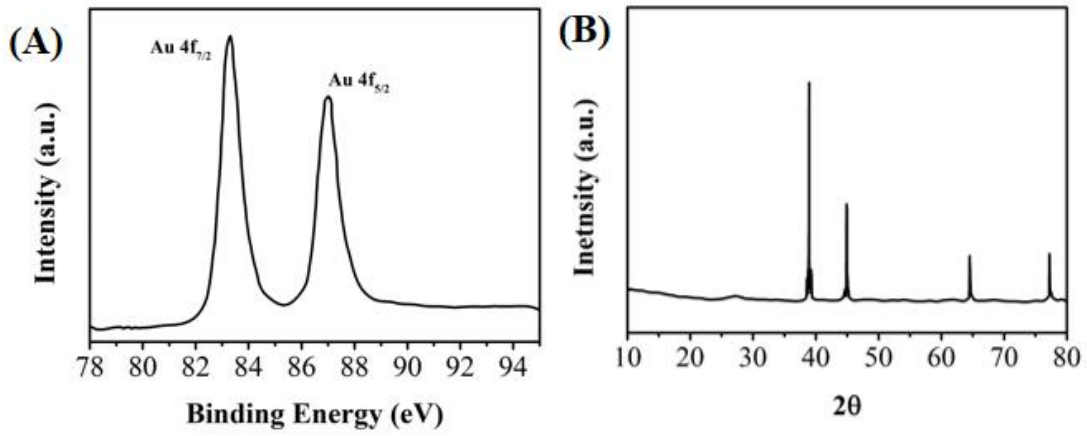

Figure 4. (A) High resolution Au 4f scan and (B) XRD pattern of biosynthesized Au nanoparticles.

The CV scans of bare SPE and biosynthesized Au nanoparticles modified SPE were used for comparing the surface active area of both electrodes. Figure 5A shows the CV scans of bare SPE and Au/SPE in the 0.5 M H_2SO_4. The scan background of the Au/SPE was clearly larger than that of the bare SPE, indicating the biosynthesized Au nanoparticles modification could largely enhance the electrode surface area. The interface properties of the bare SPE and Au/SPE were also investigated using EIS. Figure 5B shows the Nyquist plots of both electrodes. It can be seen that a much smaller semicircle in the high frequency region was observed on the Au/SPE compared with that of bare SPE, indicating that the biosynthesized Au nanoparticles modification can effectively decrease the electron transfer resistance. Randle equivalent circuit mode was used for calculating the electron transfer resistance and found to be 400 and 125 Ω for bare SPE and Au/SPE, respectively. Moreover, the concentration of the electroactive substance on Au/SPE could be further calculated using Laviron equations and found to be 9.52×10^{-5} μM/cm [47].

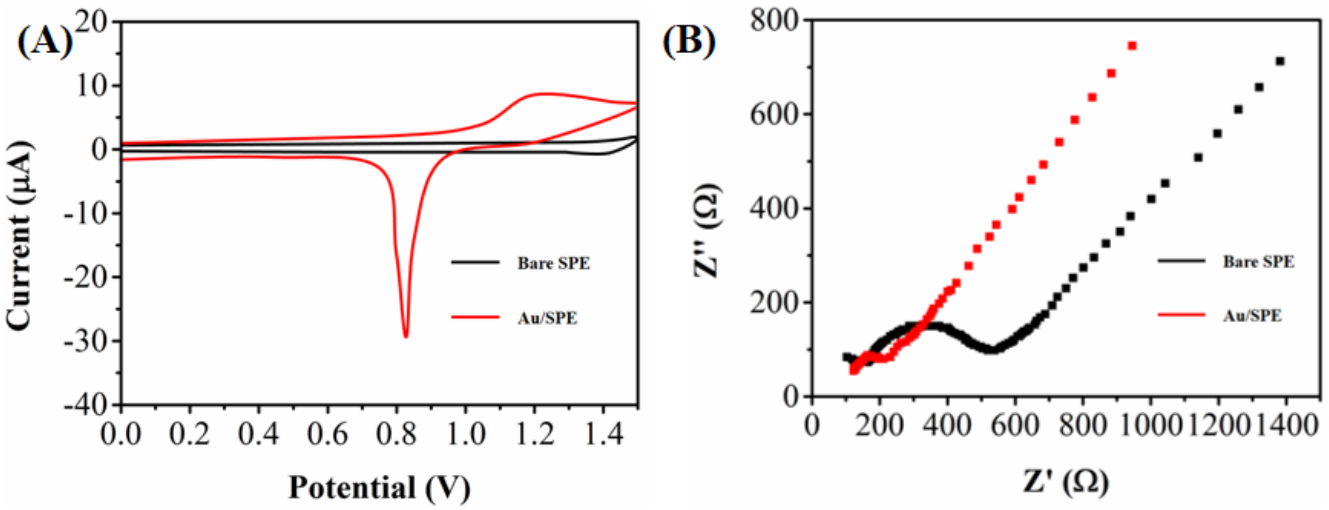

Figure 5. (A) CVs representing of bare SPE and Au/SPE electrodes in 0.5 M H_2SO_4, scan rate: 50 mV/s. (B) Nyquist plots of bare SPE and Au/SPE electrodes in the presence of 5 mM $Fe(CN)_63^{-/4-}$ with 0.1 M KCl.

Figure 6A shows the CV profiles of the bare SPE and biosynthesized Au nanoparticles modified SPE in the absence and presence of 1 μM of carbendazim. As shown in the figure, the electro-oxidation of the carbendazim was very weak at bare SPE with potential of 0.95 V. In contrast, a much higher current response was observed on the Au/SPE. The CV scan of Au/SPE at PBS without carbendazim showed no peak response, indicating the peak at 0.77 V responded to the electro-oxidation of carbendazim. The oxidation peak potential shift can be ascribed to the electrocatalytic activity of the biosynthesized Au nanoparticles, which lower the over potential of the oxidation. Therefore, the biosynthesized Au nanoparticles showed a superior performance towards detection of carbendazim.

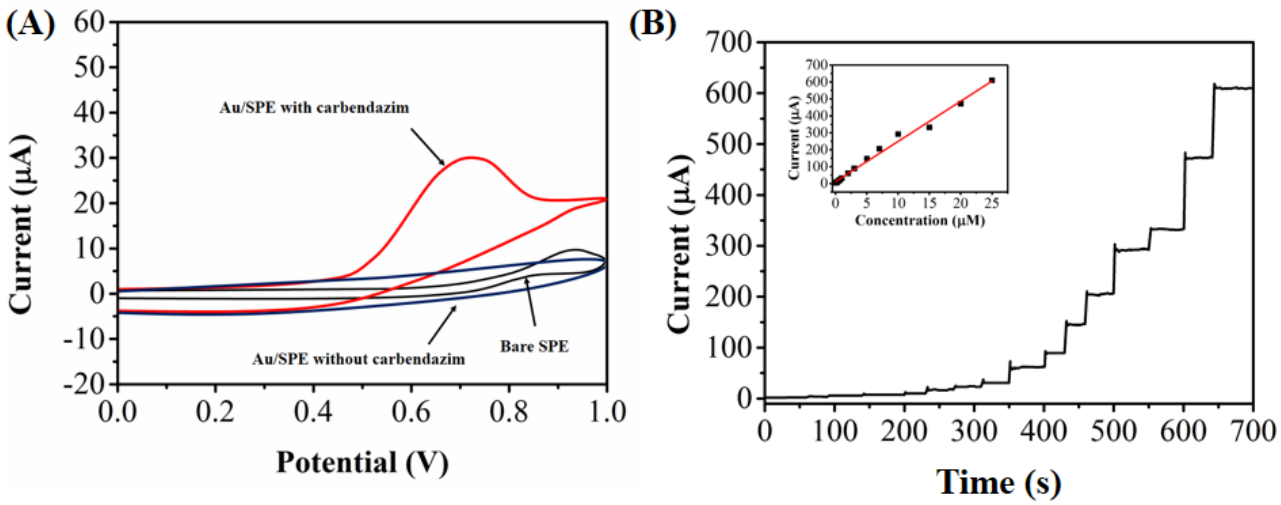

Figure 6. (A) CVs representing of bare SPE and Au/SPE electrodes toward 1 μM carbendazim in PBS. Scan rate: 50 mV/s. (B) Amperometric response of the Au/SPE with successive additions of carbendazim into PBS. Measured at 0.77 V. Inset: Magnification of current responds from 0.05 to 25 μM.

Table 1. Comparison of proposed carbendazim electrochemical sensor with other reports.

Electrode	LDR (μM)	LOD (μM)	Reference
Graphene oxide/GCE	1-100	0.5	[48]
Pyrrolidinium ionic liquid modified ordered mesoporous carbon	1.25-800	0.5	[49]
SiO_2/MWCNT	0.2-4	0.056	[50]
Diamond electrode	0.5-15	0.03	[51]
Electrochemically reduced graphene oxide/GCE	0.002-0.4	0.001	[52]
GO–MWNT/GCE	0.01-10	0.005	[53]
MWCNT-polymeric methyl red film	0.2-100	0.009	[54]
Cyclodextrin–graphene/GCE	0.005-0.25	0.002	[55]
Biosynthesized Au/SPE	0.05-25	0.0029	This work

Figure 6B shows the amperometric response of the biosynthesized Au nanoparticles towards successive addition of carbendazim. It can be seen that the Au/SPE responded very quickly after addition of the carbendazim, which can reach to the steady-state in 4 s. A linear relationship was obtained for carbendazim concentrations and current responses (Inset of Figure 6B). The proposed Au/SPE sensor could linearly response to the carbendazim from 0.05 μM to 25 μM. The detection limit can be estimated to be 2.9 nM based on the signal to noise ratio of 3. Table 1 shows the comparison of our proposed carbendazim electrochemical sensor with some previously reported sensor. Results indicated that the biosynthesized Au nanoparticles modified SPE showed a comparable performance towards carbendazim detection compared with other works.

The application of biosynthesized Au nanoparticles modified SPE was used for analyzing the trace amount of carbendazim in soil sample. We collected two soil sample from the cultivated land for

real environmental sample test. Table 2 shows the results of carbendazim content in the two real soil samples. It can be seen that the biosynthesized Au nanoparticles modified SPE showed excellent detection performances for soil samples. Therefore, the proposed carbendazim electrochemical sensor based on the biosynthesized Au nanoparticles could be used for real carbendazim determination of various environmental samples.

Table 2. Determination of carbendazim in soil sample using biosynthesized Au nanoparticles modified SPE.

Sample	Added (μM)	Found (μM)	Recovery (%)
Soil sample 1	0	0	—
	0.5	0.502	100.4
	1	1.002	100.2
	2	2.004	100.2
Soil sample 2	0	0.012	—
	0.1	0.111	100.1
	0.2	0.219	103.3
	0.5	0.515	100.6

4. CONCLUSIONS

In this contribution, we proposed a biosynthesis method towards Au nanoparticles preparation using *Pithophora oedogonia* as reducing agent. Spherical Au nanoparticles were synthesized with an average diameter of 33 nm. The biosynthesized Au nanoparticles showed a promising activity towards carbendazim determination. The linear detection range has been found to be 0.05-25 μM. The detection limit of the proposed sensor was 2.9 nM. Moreover, the proposed electrochemical carbendazim sensor was successfully applied for carbendazim detection in real soil samples.

References

1. A. Maleki, R. Rahimi and S. Maleki, *JICS*, 12 (2015) 191
2. A. Biswas, S. Paul and A. Banerjee, *Journal of Materials Chemistry A*, 3 (2015) 15074
3. N. Zhou, V. López-Puente, Q. Wang, L. Polavarapu, I. Pastoriza-Santos and Q.-H. Xu, *RSC Advances*, 5 (2015) 29076
4. N.S. King, L. Liu, X. Yang, B. Cerjan, H.O. Everitt, P. Nordlander and N.J. Halas, *ACS nano*, 9 (2015) 10628
5. S.R. Suryawanshi, V. Kaware, D. Chakravarty, P.S. Walke, M.A. More, K. Joshi, C.S. Rout and D.J. Late, *RSC Advances*, 5 (2015) 80990
6. C. Constantinescu, A. Rotaru, A. Nedelcea and M. Dinescu, *Mat. Sci. Semicon. Proc.*, 30 (2015) 242
7. J. Yang, D. Yan and T.S. Jones, *Chemical reviews*, 115 (2015) 5570
8. M. Grujicic, R. Yavari, J. Snipes and S. Ramaswami, *Journal of Materials Science*, 50 (2015) 2019
9. M. Grujicic, R. Yavari, J. Snipes and S. Ramaswami, *International Journal of Structural Integrity*,

6 (2015) 367
10. K. Roy, M.N. Alam, S.K. Mandal and S.C. Debnath, *Journal of Sol-Gel Science and Technology*, 73 (2015) 306
11. A. Gurlo, E. Ionescu, R. Riedel and D.R. Clarke, *Journal of the American Ceramic Society*, 99 (2016) 281
12. P. Hartemann, P. Hoet, A. Proykova, T. Fernandes, A. Baun, W. De Jong, J. Filser, A. Hensten, C. Kneuer and J.-Y. Maillard, *Materials Today*, 18 (2015) 122
13. S. Müller and M. Türk, *The Journal of Supercritical Fluids*, 96 (2015) 287
14. C. Sarkar and H. Hirani, *International Journal of Scientific Engineering and Technology*, 4 (2015) 76
15. D.S. Read, M. Matzke, H.S. Gweon, L.K. Newbold, L. Heggelund, M.D. Ortiz, E. Lahive, D. Spurgeon and C. Svendsen, *Environmental Science and Pollution Research*, (2015) 1
16. M.E. Bruno, M. Sittner, R.L. Cabrini, M.B. Guglielmotti, D.G. Olmedo and D.R. Tasat, *Journal of Biomedical Materials Research Part A*, 103 (2015) 471
17. A.M. Darwish, W.H. Eisa, A.A. Shabaka and M.H. Talaat, *Spectrochimica Acta Part A: Molecular and Biomolecular Spectroscopy*, 153 (2016) 315
18. M. Masnadi, N. Yao, N. Braidy and A. Moores, *Langmuir*, 31 (2015) 789
19. A. Khazaei, M. Khazaei and S. Rahmati, *J. Mol. Catal. A: Chem.*, 398 (2015) 241
20. G. Li, S. Yao, J. Zhu, C. Liu and W. Xing, *Journal of Power Sources*, 278 (2015) 9
21. H. Wei, K. Rodriguez, S. Renneckar, W. Leng and P.J. Vikesland, *The Analyst*, 140 (2015) 5640
22. N. Krasteva, I. Besnard, B. Guse, R.E. Bauer, K. Müllen, A. Yasuda and T. Vossmeyer, *Nano Letters*, 2 (2002) 551
23. B. Puértolas, Á. Mayoral, R. Arenal, B. Solsona, A. Moragues, S. Murcia-Mascaros, P. Amorós, A.B. Hungría, S.H. Taylor and T. García, *ACS Catalysis*, 5 (2015) 1078
24. X. Chen, D. Li, G. Li, L. Luo, N. Ullah, Q. Wei and F. Huang, *Appl. Surf. Sci.*, 328 (2015) 444
25. A. Jayalekshmi and C.P. Sharma, *Colloids and Surfaces B: Biointerfaces*, 126 (2015) 280
26. R. Das, S. Upadhyay, M.K. Sharma, M. Shaik, V. Rao and D.N. Srivastava, *RSC Advances*, 5 (2015) 48147
27. C. Hou, G. Meng, Z. Huang, B. Chen, C. Zhu and Z. Li, *Electrochemistry Communications*, 60 (2015) 104
28. K.W. Kim, W. Song, M.W. Jung, M.-A. Kang, S.Y. Kwon, S. Myung, J. Lim, S.S. Lee and K.-S. An, *Carbon*, 82 (2015) 96
29. P. Kuppusamy, S.J. Ichwan, N.R. Parine, M.M. Yusoff, G.P. Maniam and N. Govindan, *Journal of Environmental Sciences*, 29 (2015) 151
30. B.D. Sawle, B. Salimath, R. Deshpande, M.D. Bedre, B.K. Prabhakar and A. Venkataraman, *Science and Technology of Advanced Materials*, (2016)
31. R.M. Tripathi, R.K. Gupta, A.S. Bhadwal, P. Singh, A. Shrivastav and B. Shrivastav, *Nanobiotechnology, IET*, 9 (2015) 178
32. Y. Zheng, A. Wang, H. Lin, L. Fu and W. Cai, *RSC Advances*, 5 (2015) 15425
33. Y. Zheng, L. Fu, A. Wang, F. Peng, J. Yang and F. Han, *Sensor Letters*, 13 (2015) 878
34. Y. Zheng, L. Fu, A. Wang and W. Cai, *Int. J. Electrochem. Sci*, 10 (2015) 3530
35. Y. Zheng, L. Fu, F. Han, A. Wang, W. Cai, J. Yu, J. Yang and F. Peng, *Green. Chem. Lett. Rew.*, 8 (2015) 59
36. S. Xu, L. Fu, T.S.H. Pham, A. Yu, F. Han and L. Chen, *Ceram. Int.*, 41 (2015) 4007
37. L. He, L. Fu and Y. Tang, *Catalysis Science & Technology*, 5 (2015) 1115
38. F. Han, H. Li, J. Yang, X. Cai and L. Fu, *Physica. E*, 77 (2016) 122
39. L. Fu, D. Zhu and A. Yu, *Spectrochimica Acta Part A: Molecular and Biomolecular Spectroscopy*, 149 (2015) 396
40. L. Fu, Y.-H. Zheng and Z.-X. Fu, *Chemical Papers*, 69 (2015) 655
41. L. Fu, Y. Zheng, A. Wang, W. Cai and H. Lin, *Food chemistry*, 181 (2015) 127

42. J.-L. Jia, H.-H. Xu, L. Zhu, W.-H. Ye and D.-Q. Li, *Journal of nanoscience and nanotechnology*, 15 (2015) 1674
43. H.M. Magdi and B. Bhushan, *Microsystem Technologies*, 21 (2015) 2279
44. S.R. Tetgure, A.U. Borse, B.R. Sankapal, V.J. Garole and D.J. Garole, *Amino acids*, 47 (2015) 757
45. R. Leppelt, B. Schumacher, V. Plzak, M. Kinne and R. Behm, *J. Catal.*, 244 (2006) 137
46. J. Li, C.-y. Liu and Y. Liu, *Journal of Materials Chemistry*, 22 (2012) 8426
47. E. Laviron, *Journal of Electroanalytical Chemistry and Interfacial Electrochemistry*, 52 (1974) 355
48. S.-x. LUO, H.-y. ZHANG, Y.-h. WU and F. ZHANG, *Science and Technology of Food Industry*, 18 (2012) 011
49. Y. Ya, T. Wang, L. Xie, J. Zhu, L. Tang, D. Ning and F. Yan, *Analytical Methods*, 7 (2015) 1493
50. C.A. Razzino, L.F. Sgobbi, T.C. Canevari, J. Cancino and S.A.S. Machado, *Food Chemistry*, 170 (2015) 360
51. R.F. França, H.P.M. de Oliveira, V.A. Pedrosa and L. Codognoto, *Diamond and Related Materials*, 27–28 (2012) 54
52. X.-Y. Dong, B.-J. Qiu, X.-W. Yang, D. Jiang and K. Wang, *Electrochemistry*, 82 (2014) 1061
53. S. Luo, Y. Wu and H. Gou, *Ionics*, 19 (2013) 673
54. J. Li and Y. Chi, *Pesticide Biochemistry and Physiology*, 93 (2009) 101
55. Y. Guo, S. Guo, J. Li, E. Wang and S. Dong, *Talanta*, 84 (2011) 60